**Canadian Journal of Fisheries and Aquatic Sciences**
2017, Volume 74, Issue 7, Pages 987-999
http://dx.doi.org/10.1139/cjfas-2016-0214
http://archimer.ifremer.fr/doc/00360/47095/




# Cause or consequence? Exploring the role of phenotypic plasticity and genetic polymorphism in the emergence of phenotypic spatial patterns of the European eel

Mateo Maria [1], Lambert Patrick [1], Tétard Stéphane [2], Castonguay Martin [3], Ernande Bruno [4], Drouineau Hilaire [1]

[1] Irstea, UR EABX Ecosystèmes aquatiques et changements globaux, HYNES, France
[2] EDF R&D, HYNES Irstea – EDF R&D, Laboratoire National d'Hydraulique et Environnement, France
[3] Ministère des Pêches et des Océans, Institut Maurice-Lamontagne, Canada
[4] IFREMER, Laboratoire Ressources Halieutiques de Boulogne, France

Email addresses : Email: maria.mateo@irstea.fr ; patrick.lambert@irstea.fr ; stephane.tetard@edf.fr ; Martin.Castonguay@dfo-mpo.gc.ca ; bruno.ernande@ifremer.fr ; hilaire.drouineau@irstea.fr

**Abstract :**

The European eel (Anguilla anguilla), and generally, temperate eels, are relevant species for studying adaptive mechanisms to environmental variability because of their large distribution areas and their limited capacity of local adaptation. In this context, GenEveel, an individual-based optimization model, was developed to explore the role of adaptive phenotypic plasticity and genetic-dependent habitat selection, in the emergence of observed spatial life-history traits patterns for eels. Results suggest that an interaction of genetically and environmentally controlled growth may be the basis for genotype-dependent habitat selection, whereas plasticity plays a role in changes in life-history traits and demographic attributes. Therefore, this suggests that those mechanisms are responses to address environmental heterogeneity. Moreover, this brings new elements to explain the different life strategies of males and females. A sensitivity analysis showed that the parameters associated with the optimization of fitness and growth genotype were crucial in reproducing the spatial life-history patterns. Finally, it raises the question of the impact of anthropogenic pressures that can cause direct mortalities but also modify demographic traits, and act as a selection pressure.

**Keywords** : phenotypic plasticity, Anguilla anguilla, genetic polymorphism, life history theory, modeling

## 2 Introduction

Life-history theory posits that the schedule and duration of life-history traits are the result of natural selection to optimize individual fitness (Clark 1993; Giske et al. 1998). Optimal solutions greatly depend on environmental conditions, and consequently, living organisms have developed different adaptive mechanisms to address environmental variability. Among them, local adaptation theory posits that natural selection favors the most well adapted genotypes in each type of environment. In a context of limited genetic exchange between environments, this may lead to isolation and speciation (Williams 1996; Kawecki and Ebert 2004). Phenotypic plasticity might also be an adaptive response to an heterogeneous environment (Levins 1963; Gotthard and Nylin 1995; Pigliucci 2005). Phenotypic plasticity refers to the possibility of a genotype to produce different phenotypes depending on environmental conditions. In some cases, increases in fitness occur because of plastic phenotypes compared to non-plastic ones, and that consequently, phenotypic plasticity may be selected by natural selection (Schlichting 1986; Sultan 1987; Travis 1994).

Adaptation to environment heterogeneity is a key issue for temperate anguilids, *Anguilla anguilla*, *A. japonica*, *A. rostrata,* three catadromous species that display remarkable similarities in their life-history traits (Daverat et al. 2006; Edeline 2007). The European eel (*A. anguilla*) is widely distributed from Norway to Morocco, grows in contrasting environments, and displays considerable phenotypic variation. The species displays a complex life cycle: reproduction takes place in the Sargasso Sea, larvae (or leptocephali) are transported by ocean currents to European and North African waters, where they experience their first metamorphosis to become glass eels. These juveniles colonize continental waters and undergo progressive pigmentation changes to become yellow eels. The growth phase lasts between 2 and 20 years depending upon the region and sex of the eels (Vollestad 1992). At the end of this stage, yellow eels metamorphose again into silver eels, which mature during the migration to their spawning area in the Sargasso Sea. The population is panmictic, resulting in a homogeneous population, from a genetic viewpoint (Palm et al. 2009; Als et

al. 2011; Côté et al. 2013). This panmixia combined with a long and passive larval drift limit the possibility of adaptation to local environments. However, spatial patterns of different life traits, including growth rate (Daverat et al. 2012; Geffroy and Bardonnet 2012), sex (Helfman et al. 1987; Tesch 2003; Davey and Jellyman 2005), length at maturity (Vollestad 1992; Oliveira 1999), and habitat use (De Leo and Gatto 1995; Daverat et al. 2006; Edeline 2007) are observed and correlated with environmental patterns.

Growth rates greatly vary depending on latitude, temperature, sex (Helfman et al. 1987) but also on habitat characteristics (Cairns et al. 2009). Indeed, eel can settle in a wide range of habitats (De Leo and Gatto 1995; Daverat et al. 2006; Geffroy and Bardonnet 2012) and faster growth is observed in brackish waters than in freshwater (Daverat et al. 2012). Slower growth in freshwater habitats is sometimes assumed to be compensated for by lower mortalities and Edeline (2007) suggested that habitat choice could be the result of a conditional evolutionary stable strategy. However, Cairns et al. (2009) questioned this assumption because they did not observe strong variation in mortality rates between habitats. Spatial patterns were also observed with respect to sex ratios, with female biased sex ratios in the upper part of river catchments (Tesch 2003) and in the northern part of the distribution range (Helfman et al. 1987; Davey and Jellyman 2005). However, sex is not determined at birth but is determined by environmental factors (Oliveira 2001; Davey and Jellyman 2005; Geffroy and Bardonnet 2012). Population density also plays a role in this mechanism: males are favored at high densities, whereas low densities favor females (Tesch 2003). This is important because males and females have different life-history strategies (Helfman et al. 1987). The reproductive success of a male does not vary with body size, and consequently, males are assumed to follow a time-minimizing strategy, leaving continental waters as soon as they have enough energy to migrate to the spawning grounds (Vollestad 1992). However, a female's reproductive success is constrained by a trade-off between fecundity, which increases with length, and survival, which decreases with length. Consequently, females are assumed to adopt a size-maximizing strategy

(Helfman et al. 1987). Strong differences in female length at silvering were observed among habitats and latitudes (Oliveira 1999).

Because local adaptation is impossible, this raises two questions: (i) are those life-history trait patterns resulting from an adaptive response to environmental heterogeneity, and (ii) which adaptation mechanisms have been selected. Despite panmixia, previous researchers (Gagnaire et al. 2012; Ulrik et al. 2014; Pavey et al. 2015) have detected genetic differences correlated with environmental gradients and assumed that those differences were reshuffled at each generation because of panmixia. Common garden experiments have been used to test the respective contributions of genetic and plastic mechanisms on phenotypic differences observed in glass eels found in distinct locations. The results revealed genetic patterns related to geographic zones in American eels, whereas individual growth rates had a genetic basis and could be sex-dependent (Côté et al. 2009, 2014, 2015). Building on this, Boivin et al. (2015) studied the influence of salinity preferences and geographic origin on habitat selection and growth in American eels, demonstrating genetic-based differences for growth between glass eels from different origins. However, these experiments also confirmed the contribution of phenotypic plasticity that allowed individuals to develop quick and effective responses to environmental variability (Hutchings et al. 2007). Several traits have been proposed as plastic: growth habitats (Daverat et al. 2006; Edeline 2007), growth rates (Geffroy and Bardonnet 2012), and length at silvering (Vollestad 1992). Understanding the adaptive mechanisms that explain this diversity is crucial to environmental conservation and management (Brodersen and Seehausen 2014).

As a result of a decline observed since the 1980s, the European eel is now listed as critically endangered in the IUCN Red List (Jacoby and Gollock 2014) and the European Commission enforced a European Regulation, which requires a reduction in all sources of anthropogenic mortality (obstacles, loss of habitat, fisheries, pollution, and global change) (Council of the European Union 2007). However, those anthropogenic pressures are not uniformly distributed (Dekker 2003) and acts on specific fractions of the stock isolated in river catchments (Dekker 2000), with heterogeneous life-

history traits because of the spatial phenotypic variability. This strong spatial heterogeneity of anthropogenic pressures affecting the eel population in Europe combined with this spatial phenotypic variability at both the distribution area and river catchment scales causes specific challenges for management, because it impairs our ability to assess the effect of anthropogenic pressures on the whole stock and to coordinate management actions (Dekker 2003, 2009).

Recently, a model called EvEel (evolutionary ecology-based model for eel) was developed to explore the contribution of adaptive phenotypic plasticity in the emergence of observed phenotypic patterns: sex ratio, length at silvering, and habitat use (Drouineau et al. 2014). Assuming fitness maximization, the model was able to mimic most observed patterns at both river catchment and distribution area scales. The result confirmed the probable role of adaptive phenotypic plasticity in response to environmental variability. However, recent findings demonstrated the existence of genetic differences in growth traits in a wide range of different habitats (Côté et al. 2009, 2014, 2015; Boivin et al. 2015). Building on these new results, we developed GenEveel, a new version of EvEel, which introduces a bimodal growth distribution (fast and slow growers) for individuals, as observed by Côté et al. (2015), and considers phenotypic plasticity in life-history traits and demographic attributes as in EvEel. Because individuals have different intrinsic growth and mortality rates, they can be favored differently among environments, opening the door to conditional habitat selection. In this study, we used GenEveel to test whether simultaneously considering genetically distinct individuals and phenotypic plasticity improves model performance. Pattern orienting modelling was used to detect the reproduced spatial patterns of EvEel and other patterns based on the distribution of the different individual's types.

# 3 Materials and methods

## *3.1 Model description*

The model description follows the Overview, Design concepts, and Details (ODD) protocol (Grimm et al. 2006, 2010):

### 3.1.1 Overview

#### 3.1.1.1 Purpose

GenEveel is a model based on a former model called EvEel (Drouineau et al. 2014), but includes a genetic component. It is an individual-based population model that predicts emergent life-history spatial patterns depending on adaptive mechanisms and environmental heterogeneity. Emergent patterns can later be compared to observed spatial patterns in freshwater life stages of European eels in order to (i) confirm that observed phenotypic patterns can plausibly result from adaptive responses to environmental heterogeneity, (ii) validate that phenotypic plasticity for length at silvering, sex determination, habitat choice, and genetic polymorphism (slow growers and fast growers) with conditional habitat selection can explain those patterns.

#### 3.1.1.2 State variables and scales

*Temporal scales:* the model simulates a population generation. It has no *sensu stricto* time steps, but rather successive events: sex-determination and habitat selection, survival, and growth until maturation.

*Entities and spatial scales:* a Von Bertalanffy growth function is assumed for individual growth. Each individual *i* is characterized by an intrinsic Brody growth coefficient $K_i$ and a natural mortality rate $M_i$. Based on Côté et al. (2015), who observed two clusters in growth rates, we build a simple quantitative-genetic model assuming that growth is coded for by a single gene with two variations. Therefore, we assumed that there are two types of individuals called (i) fast-growing

individuals for which *Ki = Kfast* and *Mi = Mfast* and (ii) slow-growing individuals for which *Ki = Kslow* and *Mi = Mslow*. At the end of the simulation, individuals are characterized by a sex, length at silvering, corresponding fecundity (if female), position in the river catchment, and survival rate until silvering.

The river catchment environment was represented by a sequence of cells of the same size. The first cell represents the river mouth, whereas the *n*th cell represents the source of the river. Because it was observed that an individual grows faster downstream than upstream (Acou et al. 2003; Melià et al. 2006), we assumed that realized growth rate in a cell depends on both intrinsic growth rate and position in the catchment (i.e., cell) (see submodel section). Realized natural mortalities depend both on individual intrinsic mortality rates, position of the cell in the catchment, and number of individuals in the catchment (to mimic density-dependent mortality).

#### 3.1.1.3 Process overview and scheduling

The model has two main steps. In a first step, individuals select their growth habitat (a cell in the catchment) and determine a sex (male or female) one after another (random order). To do that, fitness is calculated for each combination of sex and cell (a quasi-Newton algorithm is used to estimate the lengths at silvering that optimize female fitness in each cell). Individuals are assumed to select the combination with highest fitness given the choices made by former individuals. Once this step is finished (i.e., all individuals have a growth habitat and sex), using the quasi-Newton algorithm we estimated the optimal length at silvering for all females (males have a constant length at silvering) given the positions of fishes from step 1, and then compute corresponding survival rates until silvering and fecundity determination (Fig. 1). The process mentioned above is defined by the computer algorithm (Figure 2):

(1) For each individual i:

- For each cell *x*:

· Compute $\pi_m(x)$ given positions of individuals *{1,…,i-1}*

197 · Compute $\max_{Ls_f} \pi_f(x, Ls_f)$ given positions of individuals *{1,…,i-1}*

198 - Put individual and determine sex by selecting maximum values within $\max_{Ls_f} \pi_f(x, Ls_f)$ and $\pi_m(x)$

199 (2) For each individual i:

200 - For each cell *x*:

201 · if sex(i) = male

202 $L_s(i) = L_{sm}$

203 · else

204 $L_s(i) = arg_L \, max \, (\pi_f(x, L_{sf}))$ given positions of individuals *{1,…,n}*

205 where fitness is defined in equations 9 and 10 for females and males respectively.

## 206 3.1.2 Design concept

### 207 3.1.2.1 Basic principles

208 Consistent with life-history theory and optimal foraging theory, the model uses an
209 optimization approach in which individuals "respond to choices" so as to select and fix the adaptive
210 traits, maximizing their expected fitness given their environment (Parker and Maynard Smith 1990;
211 McNamara and Houston 1992; Giske et al. 1998; Railsback and Harvey 2013).

### 212 3.1.2.2 Emergence

213 Using the pattern-oriented modelling approach (Grimm and Railsback 2012), GenEveel
214 compares predicted spatial patterns with those observed in real river catchments. Five emergent
215 population spatial patterns were analyzed from the literature:
216 (i) higher density downstream than upstream
217 (ii) higher length at silvering upstream than downstream
218 (iii) male-biased sex ratio downstream and female-biased sex ratio upstream

(iv) more individuals characterized with the fast-growing genotype downstream than upstream, which was mainly characterized by the slow-growing genotype

(v) the phenotypic response led to faster growth rate downstream than upstream.

#### 3.1.2.3 Adaptation

Individuals have three adaptive traits: sex-determination, length at silvering for females, and choice of growth habitat (cell in the grid). These traits are assumed to maximize the predicted objective function (i.e., the individual fitness).

#### 3.1.2.4 Predictions

We assumed that individuals could perfectly predict expected fitness given previous choices and could make the most appropriate choices.

#### 3.1.2.5 Sensing

In the model, individuals are able to "sense" fitness, which was a function of a density-dependent mortality and growth rate. In the real world, temperature and density would probably be the proximal cues because natural mortality and growth rates are strongly influenced by temperature (Bevacqua et al. 2011; Daverat et al. 2012).

#### 3.1.2.6 Interaction

Interactions occurred through growth habitat selection, sex determination, and density-dependent mortality.

#### 3.1.2.7 Stochasticity

Stochasticity occurred at two levels. First, individuals were randomly affected by a slow-growing genotype (Pr = 0.5) or by a fast-growing genotype (Pr = 0.5). Then stochasticity occurred in the order of individuals for step 1.

#### 3.1.2.8 Observations

Five spatial patterns were computed at the end of the simulation:

(i) number of individuals per cell

(ii) mean length at silvering per cell

(iii) sex ratio (proportion of females) per cell

(iv) ratio of fast-growing genotype per cell

(v) phenotypic response of mean realized growth rate per cell.

These five patterns corresponded to five patterns available in the literature. Simulated patterns (i), (iv), (v) was said to be consistent with the literature when a negative trend from downstream to upstream was observed, whereas patterns (ii), (iii) were said to be consistent with the literature when a positive trend was observed from downstream to upstream.

### 3.1.3 Details

#### 3.1.3.1 Initialization

At the beginning of the simulation, the catchment was empty. *N* individuals were created and attributed to the slow-growing or fast-growing genotype with probability 0.5 and had a length 7.5 cm. They had not yet entered the river catchment.

#### 3.1.3.2 Input data

We tested the model using a reference simulation. Values of parameters were obtained from the literature (Table 1). The outputs of the model were identified based on spatial patterns as previously defined in *Observations*.

### 3.1.3.3 Submodels

Most of the submodels were similar to submodels from EvEel. Consequently, we provide here only the novelties and the equations that are required for a better understanding of the model. Further details are provided in (Drouineau et al. 2014).

- Growth and silvering

Growth rate was assumed the outcome of an intrinsic Brody growth coefficient (*Ki*), which is modulated by an environmental effect. This combination resulted in a phenotypic growth rate. Within the river, growth rates were significantly faster downstream than upstream (even for the same individual). Therefore, we assumed that individual *i* would have a growth rate *K(i, x)* in cell *x* given by:

(1) $$K(\mathrm{i},\mathrm{x}) = r_K \cdot K(\mathrm{i},\mathrm{n}) + \left(K(\mathrm{i},1) - r_K \cdot K(\mathrm{i},\mathrm{n})\right) \cdot \mathrm{cauchit}\left(\frac{x}{n}, \gamma_K\right)$$

(2) $$\mathrm{cauchit}\ (\mathrm{x},\ \gamma) = 1 - \frac{2}{\pi} \cdot \mathrm{atan}\left(\frac{x^2}{\gamma}\right)$$

where $r_k$ defined the ratio between upstream and downstream growth rate, *K*(i, 1) is the growth rate in cell 1, *n* is the total cells in the river catchment and *cauchit* was a mathematical function similar to the sigmoid function, but which allowed asymmetrical patterns (by modifying the parameter $\gamma$) to model, for example, a small brackish area in the downstream part of the catchment and a large freshwater zone upstream.

Individual's growth was simulated by a Von Bertalanffy function:

(3) $$L(t,i,\ x) = L_\infty \left[1 - e^{-K(i,\ x)(t\ -\ t_0)}\right]$$

where *L(t, i, x)* was the length at time *t* and $L_\infty$ and *K(i, x)*, the Von Bertalanffy parameters in cell *x* for individual *i*.

From this equation, we could calculate the time required to reach the length at silvering.

(4) $$\mathrm{As}(i,x) = \frac{1}{K(i,x)} \cdot \log\left(\frac{L_\infty - Lg}{L_\infty - \mathrm{Ls}(i,x)}\right)$$

where *Lg* was the length at recruitment and *Ls(i, x)* was the length at silvering, which was constant for males, and a fitness maximizing variable for females.

- Survival

Mortality rate was assumed the result of three factors: density-dependence, intrinsic, and *Mi* modulated by an environmental effect. Because natural mortality was sometimes assumed to be smaller upstream than downstream (Moriarty 2003; Daverat and Tomás 2006), we assumed that the instantaneous natural mortality without density-dependence in cell *x* for individual *i*, *M(i, x)* was:

(5) $$M(\mathrm{i},\mathrm{x}) = r_M \cdot M(\mathrm{i},\mathrm{n}) + \left(M(\mathrm{i},1) - r_M \cdot M(\mathrm{i},\mathrm{n})\right) \cdot \mathrm{cauchit}\left(\frac{x}{n}, \gamma_M\right)$$

where $r_m$ is the ratio between upstream and downstream instantaneous mortality rate and M(i, 1) was the natural mortality in cell 1.

To account for the additional density-dependent mortality, we assumed that natural mortality increased linearly with density with an intensity α as in EvEel:

(6) $$M_d(\mathrm{i},\mathrm{x}) = M(\mathrm{i},\mathrm{x}) + N(\mathrm{i},\mathrm{x}) \cdot \alpha$$

where *N* was the number of competitors in cell *x*. An eel was assumed a competitor if it had an intrinsic growth rate greater or equal to *Ki*. This corresponded to an asymmetric growth rate with larger individuals harassing smaller individuals. The basis of this assumption was the intraspecific competition, which leads to compete for limited resources between individuals of different sizes (Francis 1983; Juanes et al. 2002).

Given equation (4) and this survival rate, we could calculate the probability of surviving until silvering as:

(7) $$p(i,x) = \mathrm{e}^{-M_d(i,x)\mathrm{As}(i,x)} = \left(\frac{L_\infty - Lg}{L_\infty - \mathrm{Ls}(i,x)}\right)^{\frac{-M_d(i,x)}{K(i,x)}}$$

- Fitness

In any optimization model, an important component is the computation of the fitness. Because sexes adopt different life strategies, and following (Drouineau et al. 2014), we assumed sex-

specific fitness functions. Males were known to adopt a time minimizing strategy (Helfman et al. 1987), with constant length at silvering. Therefore, male fitness was proportional to survival rate until length at silvering. However, females follow a size-maximizing strategy in which length at silvering was constrained by a trade-off between survival and fecundity (Helfman et al. 1987). Consequently, we assumed that female fitness was the product of fecundity at an optimal length at silvering (based on an allometric relationship, fecundity is assumed to be a power function of length) multiplied by the probability of survival until this length at silvering. In the model, individuals were assumed to determine their sex according to the relative potential male and female fitness. To make fitness values comparable, we rescaled male fitness (which was the probability of survival) into an expectation of egg production (the scale of female fitness). To do that, we multiplied the male survival by a constant that would be similar to fertility. Hence, we had to specify a value for fertility with an order of magnitude similar to fecundity. The first solution might be to fix the fertility value equal to the fecundity of silver females having a length equal to male length at silvering. However, with this solution, female fitness will always be greater (because females can optimize their length at silvering). Consequently, fertility has to be slightly greater such that male fitness can be sometimes be greater than female fitness (but not too much, to avoid male fitness always being superior). These resulted in the following equations:

(8) $$fecundity\left(L_{s_f}(i,x)\right) = \left(a_1 + a \cdot L_{s_f}(i,x)^b\right)$$

where a1, a and b are the parameters of the allometric relationship linking fecundity and female length at silvering $L_{sf}(i, x)$ (Andrello et al. 2011; Melia et al. 2006).

(9) $$\pi_f(i,x) = fecundity\left(L_{s_f}(i,x)\right) \cdot \left[\frac{L_\infty - L_g}{L_\infty - L_{s_f}(i,x)}\right]^{\frac{-M_f(i,x)}{K(i,x)}}$$

(10) $$\pi_m(i,x) = fertility \cdot \left[\frac{L_\infty - L_g}{L_\infty - L_{s_m}(i,x)}\right]^{\frac{-M_m(i,x)}{K(i,x)}}$$

## *3.2 Model exploration*

### 3.2.1 Reference simulation

The reference simulation consisted of a simulation using parameter values in Table 1, i.e. the best set of values found in the literature. After simulating this scenario, we analyzed the different patterns. Mann-Kendall tests were implemented on each pattern to detect a monotonic upward or downward trend of the variable of interest confirming the spatial patterns previously defined. The correlation coefficient of this non-parametric test was denoted by τ.

### 3.2.2 Experimental design

Simulation design is a classical tool to explore complex models. Typically, the goal is to assess the sensitivity of results to uncertain model parameters. We developed such an experimental design to (i) assess the influence of uncertain parameters on the simulated patterns (Table 1) and (ii) derive environmental and population dynamics for all the patterns that were correctly modelled.

Seventeen uncertain parameters were identified in the model (Table 1) and they were dispatched into twelve groups: number of glass eel entering the catchment freshwater ($N$), parameters that impact the male fitness (fertility and male length at silvering, $L_{sm}$), fast growing genotype ($K_{fast}(i, 1)$ and $M_{fast}(i, 1)$), slow-growing genotype ($K_{slow}(i, 1)$ and $M_{slow}(i, 1)$), proportion of individuals that grow slowly ($propK$), intensity of density-dependence ($\alpha$), cells of river catchment ($n$), regression coefficient from fecundity at length ($b$), asymptotic length ($L_\infty$), length at recruitment ($L_g$), ratio between upstream and downstream instantaneous growth and mortality rates ($r_k$ and $r_m$), and the shape parameter of growth and mortality ($\gamma_k$ and $\gamma_m$). Groups were composed of parameters that have are assumed to influence the model in similar directions, a method called group-screening (Kleijnen 1987). A low and high value was set for each parameter around the reference value, with 20% variation (Drouineau et al. 2006; Rougier et al. 2015), except for three sets of parameters: *fertility* and $L_{sm}$(as a minimum value, *fertility* corresponded to the fecundity of a female with a length

354 at silvering equals to male length at silvering; otherwise, female fitness would always be superior to
355 male fitness), and growth genotypes (to avoid overlap between them), where the range of variation
356 was less. We then conducted a fractional factorial design of resolution V ($2^{12-4}$ = 256 combinations).
357 This kind of orthogonal designs allows to explore main effects and first order interactions without
358 confusion. To account for model stochasticity, we conducted 10 replicates for each of the 256
359 combinations leading to 2560 simulations. The five patterns were calculated for each simulation
360 producing an output table with 2560 lines (one per simulation) and five columns containing the tau
361 value of the Mann-Kendall trend tests for each pattern (a negative tau value indicates a negative
362 trend from downstream to upstream while a positive tau indicates a positive trend from downstream
363 to upstream).
364

365 # 4 Results

366 ## *4.1 Reference simulation*

367 In the reference simulation, GenEveel mimicked the five spatial patterns at the catchment
368 scale (Fig. 3) Males were concentrated in the downstream section of the river where density was
369 higher (Helfman et al. 1987; Tesch 2003; Davey and Jellyman 2005). Fast growers preferentially
370 settled in downstream habitats, whereas slow growers tended to move upstream to avoid
371 competition (De Leo and Gatto 1995; Daverat et al. 2006, 2012; Drouineau et al. 2006; Edeline 2007;
372 Geffroy and Bardonnet 2012). Regarding mean length at silvering (for males and females), a smaller
373 size at maturity was simulated in the downstream section of the river, whereas larger lengths were
374 occurred gradually throughout the catchment (Vollestad 1992; Oliveira 1999).
375 The Mann-Kendall test confirmed that the five patterns were mimicked in the simulation.
376 More specifically, negative tau values confirmed a decreasing trend for density, ratio of fast growers

377 and mean realized growth rate; while positive tau values pointed to an increasing trend for ratio of
378 females and mean length at silvering (Table 2).

## 379 *4.2 Model exploration*

380 For each combination, the 10 replicates provided the same results, confirming that the
381 patterns were not sensitive to stochasticity.

382 Interestingly, 310 simulations produced only females while 640 simulations produced only
383 males. Simulations with only females corresponded to simulation where density-dependence $\alpha$, $L_\infty$
384 and the fecundity exponent $b$ were simultaneously strong. Conversely, simulations with only males
385 corresponded to simulations with a low $b$ and a low $L_\infty$. With only one sex, it was not possible to
386 calculate a spatial trend in sex ratio and with only males, it was not possible to calculate a trend of
387 length at silvering.

388 Two questions were addressed here. In a first time, we compared the five patterns to see
389 which of those patterns were frequently mimicked and which were less frequently mimicked. Then,
390 we compared the sensitivity of the model to each group of parameters. To quantify this sensitivity to
391 a group of parameters values, we compared the number of simulations that reproduce a given
392 pattern when the group had modality (-) with the number of simulations and when the group had
393 modality (+). A strong discrepancy indicated a high sensitivity to the group of parameters.

394 The Mann-Kendall tests of spatial patterns confirmed that the simulated patterns of
395 abundance, ratio of fast growers, and mean realized growth rate were consistent with the literature
396 in each of the 2560 combinations (Table 3). This result indicates that these model outputs do not
397 depend on parameters values in the parameter space considered. Consequently, the assumptions
398 about asymmetrical density-dependence and growth genotypes were enough to simulate catchment
399 colonization.

400 Regarding length at silvering pattern, patterns were consistent in 1300 simulations of the
401 1920 simulations for which it was possible to calculate a pattern (Table 3, figure 4 for several

examples). This meant that, in situations where some females were produced, the pattern was consistent in about 2/3 of the simulations. Length at silvering pattern appeared to be sensitive to most of the parameters. The two most important were $L_\infty$ and $b$: consistent pattern were much more frequent with a modality (+) (respectively 990 and 940 simulations) for these two parameters than with modality (-) (respectively 310 and 360 simulations). This is not surprising since with modality (-) for those parameters, the model produced only males in 640 simulations. Two other groups of parameters had a strong influence: male fertility/ male length at silvering and density-dependence. Consistent patterns were more frequent with low male fertility and length at silvering (800 with modality (-) vs 500 with modality (+)), and with limited density dependence (810 with modality (-) vs 490 with modality (+)).

For the female ratio pattern, 130 simulations produced consistent patterns over the 1610 simulations for which it was possible to calculate a pattern (Table 3). This pattern was mostly sensitive to four groups of parameters which correspond to the four most influential groups for the pattern of length at silvering. Patterns were consistent only when male fertility/length at silvering had modality (-) whereas Kslow/Mslow had modality (+). Moreover, consistent patterns were more frequent when $L_\infty$ had a modality (-) and $b$ a modality (+).

On the whole, 130 of the 2560 combinations produced results which were consistent for all the five patterns (Table 4, Figure 4 and Table S1). These 130 simulations corresponded exactly to the 130 simulations that produced consistent sex ratio patterns, demonstrating that this last pattern was the more constraining (Figure 5). Consequently, the interpretation regarding sensitive parameters was similar.

To make a summary of those results: in situations where females' fitness was favoured because of a strong $L_\infty$ or a strong $b$, i.e. a high fecundity, the model produced only females. Conversely, when females were too penalised, model produced only males. Therefore, an equilibrim was required between males and females fitnesses to mimic all patterns. The patterns in length at silvering and sex ratio were the two most constraining patterns and were mainly sensitive to 4

groups of patterns. These groups of parameters set the equilibrium between males and females fitnesses (male fertility and length at silvering, *b* and $L_\infty$) and the advantages between slow and fast growers. Density-dependence was also important regarding the pattern on length at silvering. We cab observed that the five patterns were consistent mostly when slow growers and females were not too penalized with respect to males and fast-growers.

Some of the patterns were indeed very constrained by model assumptions so it is hardly surprising that they were mimicked by the model. For example, our constraints on mortality and growth really constrained the distribution of fishes and probably the pattern of realised growth rates in the catchment. However, those constraints were based on various observations in the literature that have rarely been considered together to see if they make sense in a context of adaptive response. We do not specify any constraints on the sex ratio, length at maturity and relationships between sex ratio and slow/fast growers. Those results are really emerging patterns that are consistent with the literature.

# 5 Discussion

## *5.1 Adaptation to environmental variability: phenotypic plasticity and genetic polymorphism of European eel*

The European eels, and more generally, temperate eels, display fascinating characteristics: catadromy with a long larval drift, large distribution area with contrasted growth habitats, panmixia, and strong phenotypic and tactic variability at different spatial scales. Consequently, this species is relevant to explore adaptive mechanisms to environmental variability. Phenotypic plasticity has been proposed as one such mechanism because of random mating and larval dispersal that prevent local selection pressures to generate habitat-specific adaptations, or local adaptation, from one generation to the next. Drouineau et al. (2014) developed the first model to explore the major role of

phenotypic plasticity in both life-history traits and tactical choices as an adaptive response to spatially structured environments and density dependence. However, recently Gagnaire et al. (2012), Pujolar et al. (2014), Boivin et al. (2015), Côté et al. (2015) and Pavey et al. (2015) demonstrated the existence of genetic differences correlated with the environment, suggesting that part of the observed phenotypic variability had a genetic basis.

Based on the approach developed by Drouineau et al. (2014), the objective of this study was to propose a model based on life-history theory and optimal foraging theory to explore the role of both adaptive phenotypic plasticity and genetic polymorphism with genetic-dependent habitat selection, in the emergence of phenotypic patterns. To that end, we used a pattern-oriented modelling approach, as developed by Grimm et al. (1996). This kind of approach compared field observed patterns to simulated patterns and postulated that those patterns are similar, the model is likely to contain the mechanisms generating these patterns.

## *5.2 In which conditions were the patterns mimicked?*

Similarly to Eveel, a main limitation of our approach was that it was based on a simulation model with a pattern-oriented approach. Consequently, our results demonstrated that our assumptions were plausible, but did not demonstrate that they were correct. Such a demonstration would require demonstrating underlying mechanisms, for example by conducting complementary controlled experiments.

We built a full experimental design to explore the model. This type of approach is classical in complex model exploration (de Castro et al. 2001, Faivre et al. 2013). For example, in the context of sensitivity analysis of complex simulation models (Drouineau et al. 2006). Our exploration goals were to generate simulations from the parameter space and analyze the qualitative differences in the model output to (i) study the impact of parameters on the model output, (ii) determine which parameters were the most important, and (iii) identify the combinations of parameters required to

476 mimic all observed spatial patterns. In this study, 17 parameters grouped in 12 set of parameters,
477 were chosen to define the region of the parameter space where all spatial patterns were reproduced.
478 To assess the influence of stochasticity, we made 10 replicates per combination. This can
479 appear limited, however, it was impossible to increase the number of simulations and we preferred
480 to have a better exploration of uncertainty due to uncertain parameters rather than on stochasticity
481 which is rather limited in our model. Stochasticity occurs during the initialization process when
482 randomly building slow or fast value with a given probability. This corresponds to a binomial
483 distribution which has, given the large number of individuals, a very small variance. Stochasticity also
484 occurs in the order of individuals for step 1, but this is closely linked to the previous process and
485 consequently also has a limited variability. This limited effect of stochasticity was confirmed by our
486 results since patterns per combination were always consistent among replicates (figure 4 and 5).
487 One hundred thirty simulations among the 2560 mimicked the five spatial patterns. The
488 fourth pattern stated that fast growers and slow growers had different spatial distributions. Fulfilling
489 this pattern demonstrated that genetically different individuals have different habitat selection
490 strategies to maximize their respective fitnesses. Consequently, fulfilling the five patterns suggested
491 that, at least in certain conditions, genotype-dependent habitat selection and phenotypic plasticity
492 could explain observed phenotypic patterns. The level of sensitivity was variable among groups of
493 parameters, but four main groups of parameters were crucial: males' fertility and length at silvering,
494 growth and mortality rates of slow growers, fecundity, and $L_\infty$. Density-dependence was also an
495 important parameter regarding length at silvering. In summary, the patterns were mimicked in
496 simulations with dominants and dominated but when dominated individuals, mainly females, were
497 not too penalized with respect to dominants, mainly males.
498 Regarding the spatial patterns, higher density, higher proportions of fast growers, and faster
499 growth rates in downstream regions were mimicked for all combinations of parameters. This
500 suggested that in the range of variation considered, none of the parameters had effects on model
501 outputs. This probably means that the gradient in environmental conditions and the population

dynamics in the model were sufficient to reproduce these patterns, regardless of the competitive advantage of fast growers with respect to slow growers, confirming that phenotypic plasticity plays an important role in environmentally induced changes in life-history traits and demographic attributes. Concerning the two other patterns (sex ratio and length at silvering), additional hypotheses are needed regarding competition and genetic polymorphism. They were fulfilled in conditions of weak competition and when growth differences were not too strong between the two genotypes.

### *5.3 Consequences with respect to intra-specific competition*

In our model, we assumed the existence of asymmetrical density dependence between fast and slow growers. We assumed that smaller individuals would avoid engaging in competition with larger ones (regardless of sex) and would consequently be more affected by density dependence. This assumption seems ecologically realistic. Asymmetrical density dependence has been observed in plants (Weiner 1990), insects (Varley et al. 1973), and fish (DingsØr et al. 2007). Intraspecific competition is a very common mechanism of density dependence, favoring large body size in fishes (Francis 1983; Juanes et al. 2002). In anguillid eels, this may be manifested through agonistic interactions (Knights 1987; Bardonnet et al. 2005), including cannibalism (Edeline and Elie 2004). Such behaviors have been observed in yellow eels under artificial rearing conditions (Peters et al. 1980; Degani and Levanon 1983; Knights 1987).

We modelled this asymmetric competition by specifying different levels of density-dependent mortality for slow and fast growers. Interestingly, the spatial patterns were still reproduced when setting these parameters to a similar value (not presented here). Indeed, even with similar intensity of density dependence, slow growers needed more time to reach their length at silvering and consequently, suffered competition longer. Thus, even if competition has the same impact on instantaneous mortality rates of slow and fast-growers, density dependence produces asymmetric impacts on their respective fitness. In EvEel, Drouineau et al. (2014) assumed the

existence of asymmetric competition between males and females, with females being more affected by competition. Interestingly, we observed in our results that females had a higher proportion of slow growers than males. This means that the gender-based asymmetry proposed by Drouineau et al. (2014) may be an indirect result of an asymmetry between two genetically distinct types of individuals with respect to growth.

The asymmetric competition implies that fitness of individuals having a given growth genotype depends on the number of individuals having the other growth genotype, which may lead to frequency-dependent selection (Heino et al. 1998). This has several implications. In the model, we assumed that individual fitness corresponded to the lifetime reproductive success called R0, and that this fitness is maximized. However, in a frequency-dependent selection context (i) natural selection does not necessarily lead in fitness maximization (Mylius and Diekmann 1995; Metz et al. 2008) and, (ii) fitness may need to be defined as an invasion criterion (Metz et al. 1992). Even when fitness maximisation applies, r, the population growth rate, may be a more appropriate measure of fitness than R0 depending on how density-dependence acts (Mylius and Diekmann 1995). To ensure that our assumptions about fitness definition and maximization were valid would require a multi-generational model at the scale of the population distribution area. This would allow computing fitness for the whole life-cycle across all potential habitat types of the distribution area while accounting for population structure in terms of genotypes or clusters. At this point, it would be interesting to explore the heritability of the different traits and the intra-generational spatially varying selection, a mechanism suggested by the SNP differences reported by (Pujolar et al. 2011; Gagnaire et al. 2012; Ulrik et al. 2014), according to latitude. This was not possible because of difficulties to develop a whole life-cycle model. More specifically, the fractal dimension of the eel population makes it very difficult to develop a population dynamics model for the continental phase at the distribution area scale. Moreover, such a model would require the use of stock-recruitment relationships, which is very difficult for the European eels because of insufficient data, long larval drift, and different recruitment trends through the distribution area. In this context, we had to use

intra-generational model and a R0 fitness function, restricted to a single catchment and a portion of the whole life-cycle, and to postulate that this R0 was maximised.

### *5.4 Reinterpreting the time-minimizing and size-maximizing strategies*

To summarize the results for combinations of parameters that mimicked observed patterns, we observed a high proportion of individuals, mainly fast growers, in the downstream environment, which corresponded to marine or brackish water. These individuals were mainly males with a constant length at silvering. In upstream areas, we found mainly slow growers, primarily females with higher length at silvering. This can aid in the reinterpretation of gender difference in life tactics (i.e., males with a time-maximizing strategy and females with a size-maximizing strategy). Our results suggest that these tactics were possibly based on the existence of two genotypes for growth. Fast growers grow fast but suffer higher mortality (because they inhabit downstream habitats with higher mortality and density); a time-minimizing strategy is suitable for them. Slow growers grow slowly but suffer lower mortality, consequently they can stay longer in continental habitats, and a size-maximizing strategy is suitable for them.

Another interesting question is whether cues are used by individuals to select their growth habitat. In the model, individuals were omnipotent and omniscient: they were able to assess the potential fitness in each cell and move in the most suitable cell. This would mean that they were able to assess the natural mortality, growth rate, and density in each cell. Drouineau et al. (2014) suggested that temperature might be one of the main proximal cue used by individuals to assess the suitability. Regarding density-dependence, reaction to aggressiveness (Geffroy and Bardonnet, 2012) or cons-specific odors (Schmucker et al. 2016) have been were observed on growth and propensity to migrate. Vélez-Espino and Koops (2010) also revealed temperature as main factor explaining variation in life-history traits. Our model suggested that density in various habitats was also probably a main cue, especially for slow growers, which tended to minimize competition.

## *5.5 Perspectives*

### 5.5.1 Exploring conditions in which phenotypic plasticity is adaptive

It has been demonstrated that phenotypic plasticity allows short-term adaptation to environmental heterogeneity for many species (Schlichting 1986; Sultan 1987; Scheiner 1993; Pigliucci 2005). However, the fitness gain arising from phenotypic plasticity should overcome its cost to be selected. This last point has not been demonstrated for eels. One possibility would be to simulate the evolution of a plastic reaction norm, for example length at silvering, close to the model developed by Marty et al. (2011). Following Ernande et al. (2004) and based on adaptive dynamics models Mylius and Diekmann (1995), it would be interesting to explore in which environmental and density-dependence conditions, phenotypic plasticity may be selected as an adaptive mechanism despite its costs, and if plasticity is still adaptive in a context of low densities after a population collapse.

### 5.5.2 Assessing the impact of anthropogenic pressures at the distribution area scale

Another perspective is to assess the impact of anthropogenic pressures on eel populations. Drouineau et al. (2014) mentioned that, because of phenotypic plasticity, anthropogenic pressures are not only a source of mortality, but may also affect sex ratio or mean length at silvering. The existence of two genotypes for growth suggests that anthropogenic activities may act as selective forces. Recently, Podgorniak et al. (2015) demonstrated that human-induced obstacles to migration could act as an evolutionary pressure. Concerning this, Boulenger et al. (2016) highlighted that human pressures impact survival, leading to different life-history strategies.

599 To conclude, our model provided new insights on eel adaptive mechanisms to heterogeneous
600 environments. Phenotypic plasticity and genotype-dependent habitat selection are two types of
601 mechanisms that can explain the patterns in life-history traits observed in natural environments at
602 the river catchment scale. A better understanding of these mechanisms is crucial to interpret the
603 observations made in the environment, the effects of anthropogenic pressures on the population,
604 and to understand if eels are still adapted in the context of depleted population size and climate
605 change.
606

## 607 6 Acknowledgements

608 This study was supported by the Hynes project between Irstea and EDF R&D. We would like
609 to thank Christian Rigaud and Laurent Beaulaton and two anonymous referees for their contribution
610 to the discussion.
611

## 612 7 References

613 Acou, A., Lefebvre, F., Contournet, P., Poizat, G., Panfili, J., and Crivelli, A.J. 2003. Silvering of female
614 eels (*Anguilla anguilla*) in two sub-populations of the Rhone Delta. Bull. Fr. Pêche Piscic. 368:
615 55–68.
616 Als, T.D., Hansen, M.M., Maes, G.E., Castonguay, M., Riemann, L., Aarestrup, K., Munk, P., Sparholt,
617 H., Hanel, R., and Bernatchez, L. 2011. All roads lead to home: panmixia of European eel in
618 the Sargasso Sea. Mol. Ecol. **20**(7): 1333–1346. doi:10.1111/j.1365-294X.2011.05011.x.
619 Andrello, M., Bevacqua, D., Maes, G.E., and De Leo, G.A. 2011. An integrated genetic-demographic
620 model to unravel the origin of genetic structure in European eel (*Anguilla anguilla* L.):
621 Genetic-demographic model for the European eel. Evol. Appl. **4**(4): 517–533.
622 doi:10.1111/j.1752-4571.2010.00167.x.
623 Bardonnet, A., Rigaud, C., and Labonne, J. 2005. Etude expérimentale des comportements de civelles
624 d'*Anguilla anguilla* L. influence de la densité et de la disponibilité en abris. Bull. Fr. Pêche
625 Piscic. **378–379**: 47–65.

626 Bevacqua, D., Melià, P., De Leo, G.A., and Gatto, M. 2011. Intra-specific scaling of natural mortality in
627 fish: the paradigmatic case of the European eel. Oecologia **165**(2): 333–339.
628 doi:10.1007/s00442-010-1727-9.
629 Boivin, B., Castonguay, M., Audet, C., Pavey, S.A., Dionne, M., and Bernatchez, L. 2015. How does
630 salinity influence habitat selection and growth in juvenile American eels *Anguilla rostrata*?:
631 salinity preference in *Anguilla rostrata* glass eels. J. Fish Biol. **86**(2): 765–784.
632 doi:10.1111/jfb.12604.
633 Boulenger, C., Acou, A., Gimenez, O., Charrier, F., Tremblay, J., and Feunteun, E. 2016. Factors
634 determining survival of European eels in two unexploited sub-populations. Freshw. Biol.
635 **61**(6): 947–962. doi:10.1111/fwb.12759.
636 Brodersen, J., and Seehausen, O. 2014. Why evolutionary biologists should get seriously involved in
637 ecological monitoring and applied biodiversity assessment programs. Evol. Appl. **7**(9): 968–
638 983. doi:10.1111/eva.12215.
639 Cairns, D.K., Secor, D.A., Morrison, W.E., and Hallett, J.A. 2009. Salinity-linked growth in anguillid eels
640 and the paradox of temperate-zone catadromy. J. Fish Biol. **74**(9): 2094–2114.
641 doi:10.1111/j.1095-8649.2009.02290.x.
642 de Castro, L.A.B., Petrere Jr., M., and Comune, A.E. 2001. Sensitivity of the BEAM4 fisheries
643 bioeconomic model to the main biological input parameters. Ecol. Model. **141**(1–3): 53–66.
644 doi:10.1016/S0304-3800(01)00241-1.
645 Clark, C.W. 1993. Dynamic Models of Behavior: An extension of Life-history Theory. Tree **8**(6): 205–
646 209.
647 Côté, C.L., Castonguay, M., Kalujnaia, M., Cramb, G., and Bernatchez, L. 2014. In absence of local
648 adaptation, plasticity and spatially varying selection rule: a view from genomic reaction
649 norms in a panmictic species (*Anguilla rostrata*). BMC Genomics **15**(1): 403.
650 doi:10.1186/1471-2164-15-403.
651 Côté, C.L., Castonguay, M., Verreault, G., and Bernatchez, L. 2009. Differential effects of origin and
652 salinity rearing conditions on growth of glass eels of the American eel *Anguilla rostrata* :
653 implications for stocking programmes. J. Fish Biol. **74**(9): 1934–1948. doi:10.1111/j.1095-
654 8649.2009.02291.x.
655 Côté, C.L., Gagnaire, P.-A., Bourret, V., Verreault, G., Castonguay, M., and Bernatchez, L. 2013.
656 Population genetics of the American eel (*Anguilla rostrata*): $F_{ST}$ = 0 and North Atlantic
657 Oscillation effects on demographic fluctuations of a panmictic species. Mol. Ecol. **22**(7):
658 1763–1776. doi:10.1111/mec.12142.

659 Côté, C.L., Pavey, S.A., Stacey, J.A., Pratt, T.C., Castonguay, M., Audet, C., and Bernatchez, L. 2015.
660 Growth, Female Size, and Sex Ratio Variability in American Eel of Different Origins in Both
661 Controlled Conditions and the Wild: Implications for Stocking Programs. Trans. Am. Fish. Soc.
662 **144**(2): 246–257. doi:10.1080/00028487.2014.975841.
663 Council of the European Union. 2007. Council Regulation (EC) No 1100/2007 of 18 September 2007
664 establishing measures for the recovery of the stock of European eel. Brussels: 7pp.
665 Daverat, F., Beaulaton, L., Poole, R., Lambert, P., Wickström, H., Andersson, J., Aprahamian, M.,
666 Hizem, B., Elie, P., Yalçın-Özdilek, S., and Gumus, A. 2012. One century of eel growth: changes
667 and implications. Ecol. Freshw. Fish **21**(3): 325–336. doi:10.1111/j.1600-0633.2011.00541.x.
668 Daverat, F., Limburg, K.E., Thibault, I., Shiao, J.-C., Dodson, J.J., Caron, F., Tzeng, W.-N., Iizuka, Y., and
669 Wickstrom, H. 2006. Phenotypic plasticity of habitat use by three temperate eel species,
670 *Anguilla anguilla*, *A. japonica* and *A. rostrata*. Mar. Ecol. Prog. Ser. **308**: 231–241.
671 Daverat, F., and Tomás, J. 2006. Tactics and demographic attributes in the European eel *Anguilla*
672 *anguilla* in the Gironde watershed, SW France. Mar. Ecol.-Prog. Ser. **307**: p–247.
673 Davey, A.J.H., and Jellyman, D.J. 2005. Sex Determination in Freshwater Eels and Management
674 Options for Manipulation of Sex. Rev. Fish Biol. Fish. **15**(1–2): 37–52. doi:10.1007/s11160-
675 005-7431-x.
676 De Leo, G.A., and Gatto, M. 1995. A size and age-structured model of the European eel (*Anguilla*
677 *anguilla* L.). Can. J. Fish. Aquat. Sci. **52**: 1351–1367.
678 Degani, G., and Levanon, D. 1983. The influence of low density on food adaptation, cannibalism and
679 growth of eels (*Anguilla anguilla* (L.)). Bamidgeh **35**: 53–60.
680 Dekker, W. 1998. Long-term trends in the glass eels immigrating at Den Oever, The Netherlands. Bull.
681 Fr. Pêche Piscic. (349): 199–214. doi:10.1051/kmae:1998045.
682 Dekker, W. 2000. The fractal geometry of the European eel stock. ICES J. Mar. Sci. **57**(1): 109–121.
683 doi:10.1006/jmsc.1999.0562.
684 Dekker, W. 2003. Status of the European Eel Stock and Fisheries. *In* Eel Biology. *Edited by* K. Aida, K.
685 Tsukamoto, and K. Yamauchi. Springer Japan. pp. 237–254.
686 Dekker, W. 2009. Worldwide decline of eel resources necessitates immediate action.
687 Desaunay, Y., and Guerault, D. 1997. Seasonal and long-term changes in biometrics of eel larvae: a
688 possible relationship between recruitment variation and North Atlantic ecosystem
689 productivity. J. Fish Biol. **51**(sA): 317–339.
690 Desaunay, Y., Lecomte-Finiger, R., and Guérault, D. 2012. Mean age and migration patterns of
691 *Anguilla anguilla* (L.) glass eels from three French estuaries (Somme, Vilaine and Adour
692 Rivers). Arch. Pol. Fish. **20**(3). doi:10.2478/v10086-012-0023-1.

693 DingsØr, G.E., Ciannelli, L., Chan, K.-S., Ottersen, G., and Stenseth, N.C. 2007. Density dependence
694 and density independence during the early life stages of four marine fish stocks. Ecology
695 **88**(3): 625–634.
696 Drouineau, H., Mahévas, S., Pelletier, D., and Beliaeff, B. 2006. Assessing the impact of different
697 management options using ISIS-Fish: the French *Merluccius merluccius* – *Nephrops*
698 *norvegicus* mixed fishery of the Bay of Biscay. Aquat. Living Resour. **19**(1): 15–29.
699 doi:10.1051/alr:2006002.
700 Drouineau, H., Rigaud, C., Daverat, F. and Lambert, P. 2014. EvEel (evolutionary ecology-based model
701 for eel): a model to explore the role of phenotypic plasticity as an adaptive response of three
702 temperate eels to spatially structured environments. Can. J. Fish. Aquat. Sci. **71**(10): 1561–
703 1571. doi:10.1139/cjfas-2014-0090.
704 Edeline, E. 2007. Adaptive phenotypic plasticity of eel diadromy. Mar. Ecol. Prog. Ser. **341**: 229–232.
705 Edeline, E., and Elie, P. 2004. Is salinity choice related to growth in juvenile eel *Anguilla anguilla*?
706 Cybium **28**: 77–82.
707 Ernande, B., Dieckmann, U., and Heino, M. 2004. Adaptive changes in harvested populations:
708 plasticity and evolution of age and size at maturation. Proc. R. Soc. Lond. B Biol. Sci.
709 **271**(1537): 415–423.
710 Faivre, R., Iooss, B., Mahévas, S., Makowski, D., and Monod, H. 2013. Analyse de sensibilité et
711 exploration de modèles. Editions Quae.
712 Francis, R.C. 1983. Experiential effects on agonistic behavior in the paradise fish, *Macropodus*
713 *opercularis*. Behaviour **85**(3): 292–313.
714 Gagnaire, P.-A., Normandeau, E., Cote, C., Moller Hansen, M., and Bernatchez, L. 2012. The Genetic
715 Consequences of Spatially Varying Selection in the Panmictic American Eel (*Anguilla*
716 *rostrata*). Genetics **190**(2): 725–736. doi:10.1534/genetics.111.134825.
717 Geffroy, B., and Bardonnet, A. 2012. Differential effects of behaviour, propensity to migrate and
718 recruitment season on glass eels and elvers' growing performance: Young eel behaviour and
719 growth pattern. Ecol. Freshw. Fish **21**(3): 469–482. doi:10.1111/j.1600-0633.2012.00566.x.
720 Giske, J., Huse, G., and Fiksen, O. 1998. Modelling spatial dynamics of fish. Rev. Fish Biol. Fish. **8**: 57–
721 91. doi:10.1023/A:1008864517488.
722 Gotthard, K., and Nylin, S. 1995. Adaptive plasticity and plasticity as an adaptation: a selective review
723 of plasticity in animal morphology and life-history. Oikos **74**(1): 3–17. doi:10.2307/3545669.
724 Grimm, V., Berger, U., Bastiansen, F., Eliassen, S., Ginot, V., Giske, J., Goss-Custard, J., Grand, T., Heinz,
725 S.K., Huse, G., Huth, A., Jepsen, J.U., Jørgensen, C., Mooij, W.M., Müller, B., Pe'er, G., Piou, C.,
726 Railsback, S.F., Robbins, A.M., Robbins, M.M., Rossmanith, E., Rüger, N., Strand, E., Souissi, S.,

727 Stillman, R.A., Vabø, R., Visser, U., and DeAngelis, D.L. 2006. A standard protocol for
728 describing individual-based and agent-based models. Ecol. Model. **198**(1–2): 115–126.
729 doi:10.1016/j.ecolmodel.2006.04.023.
730 Grimm, V., Berger, U., DeAngelis, D.L., Polhill, J.G., Giske, J., and Railsback, S.F. 2010. The ODD
731 protocol: A review and first update. Ecol. Model. **221**(23): 2760–2768.
732 doi:10.1016/j.ecolmodel.2010.08.019.
733 Grimm, V., Frank, K., Jeltsch, F., Brandl, R., Uchmanski, J., and Wissel, C. 1996. Pattern-oriented
734 modelling in population ecology. Sci. Total Environ. **183**: 155–166.
735 Grimm, V., and Railsback, S.F. 2012. Pattern-oriented modelling: a "multi-scope" for predictive
736 systems ecology. Philos. Trans. R. Soc. B Biol. Sci. **367**(1586): 298–310.
737 doi:10.1098/rstb.2011.0180.
738 Heino, M., Metz, J.A.J., and Kaitala, V. (1998). The enigma of frequency-dependent selection. Trends
739 Ecol. Evol. (13): 367–370.
740 Helfman, G.S., Facey, D.E., Stanton Hales, L., and Bozeman, E.L. 1987. Reproductive Ecology of the
741 American eel. Am. Fish Soc. Symp. **1**: 42–56.
742 Hutchings, J.A., Swain, D.P., Rowe, S., Eddington, J.D., Puvanendran, V., and Brown, J.A. 2007. Genetic
743 variation in life-history reaction norms in a marine fish. Proc. R. Soc. B Biol. Sci. **274**(1619):
744 1693–1699. doi:10.1098/rspb.2007.0263.
745 Jacoby, D., and Gollock, M. 2014. *Anguilla anguilla*. The IUCN Red List of Threatened Species.
746 Available from http://www.iucnredlist.org/details/60344/0.
747 Juanes, F., Buckel, J.A., and Scharf, F.S. 2002. Feeding ecology of piscivorous fishes. *In* Handbook of
748 fish biology and fisheries, Blackwell. Paul J.B. Hart and John D. Reynolds, UK. pp. 267–283.
749 Kawecki, T.J., and Ebert, D. 2004. Conceptual issues in local adaptation. Ecol. Lett. **7**(12): 1225–1241.
750 doi:10.1111/j.1461-0248.2004.00684.x.
751 Kleijnen, J.P.C. 1987. Statistical Tools for Simulation Practitioners. Marcel Dekker, Inc., New York, NY,
752 USA.
753 Knights, B. 1987. Agonistic behaviour and growth in the European eel, *Anguilla anguilla* L., in relation
754 to warm-water aquaculture. J. Fish Biol. **31**(2): 265–276.
755 Levins, R. 1963. Theory of fitness in a heterogeneous environment. II. Developmental flexibility and
756 niche selection. Am. Nat. **97**(893): 75–90. doi:10.1086/ 282258.
757 Marty, L., Dieckmann, U., Rochet, M.-J., and Ernande, B. 2011. Impact of Environmental Covariation
758 in Growth and Mortality on Evolving Maturation Reaction Norms. Am. Nat. **177**(4): E98–
759 E118. doi:10.1086/658988.

760 McNamara, J.M., and Houston, A.I. 1992. State-dependent life-history theory and its implications for
761 optimal clutch size. Evol. Ecol. **6**(2): 170–185. doi:10.1007/BF02270710.
762 Melià, P., Bevacqua, D., Crivelli, A.J., De Leo, G.A., Panfili, J., and Gatto, M. 2006. Age and growth of
763 *Anguilla anguilla* in the Camargue lagoons. J. Fish Biol. **68**: 876–890. doi:10.1111/j.1095-
764 8649.2006.00975.x.
765 Metz, J.A.J., Mylius, S.D., and Diekmann, O. 2008. When does evolution optimize? Evol. Ecol. Res.
766 **10**(5): 629–654.
767 Metz, J.A.J., Nisbet, R.M., and Geritz, S.A.H. 1992. How should we define "fitness" for general
768 ecological scenarios? Trends Ecol. Evol. **7**(6): 198–202.
769 Moriarty, C. 2003. The eel. *In* Eel Biology. Springer Japan, Tokyo. pp. 89–105.
770 Mylius, S.D., and Diekmann, O. 1995. On Evolutionarily Stable Life Histories, Optimization and the
771 Need to Be Specific about Density Dependence. Oikos **74**(2): 218–224.
772 Oliveira, K. 1999. Life-history characteristics and strategies of the American eel, *Anguilla rostrata*.
773 Can. J. Fish. Aquat. Sci. **56**(5): 795–802.
774 Oliveira, K. 2001. Regional variation and the effect of lake: river area on sex distribution of American
775 eels. J. Fish Biol. **58**(4): 943–952. doi:10.1006/jfbi.2000.1503.
776 Palm, S., Dannewitz, J., Prestegaard, T., and Wickström, H. 2009. Panmixia in European eel revisited:
777 no genetic difference between maturing adults from southern and northern Europe.
778 Heredity **103**(1): 82–89.
779 Parker, G.A., and Maynard Smith, J. 1990. Optimality theory in evolutionary biology. Nature **348**: 27–
780 33.
781 Pavey, S.A., Gaudin, J., Normandeau, E., Dionne, M., Castonguay, M., Audet, C., and Bernatchez, L.
782 2015. RAD Sequencing Highlights Polygenic Discrimination of Habitat Ecotypes in the
783 Panmictic American Eel. Curr. Biol. **25**(12): 1666–1671. doi:10.1016/j.cub.2015.04.062.
784 Peters, G., Delventhal, H., and Klinger, H. 1980. Physiological and Morphological Effects of Social
785 Stress on the Eel, *Anguilla anguilla* L. *In* Fish Diseases. *Edited by* D.W. Ahne. Springer Berlin
786 Heidelberg. pp. 225–227.
787 Pigliucci, M. 2005. Evolution of phenotypic plasticity: Where are we going now? Trends Ecol. Evol.
788 **20**(9): 481–486. doi:10.1016/j.tree.2005.06.001.
789 Podgorniak, T., Angelini, A., Blanchet, S., de Oliveira, E., Pierron, F., and Daverat, F. 2015. Climbing
790 experience in glass eels: A cognitive task or a matter of physical capacities? Physiol. Behav.
791 **151**: 448–455. doi:10.1016/j.physbeh.2015.08.001.
792 Pujolar, J.M., Bevacqua, D., Andrello, M., Capoccioni, F., Ciccotti, E., De Leo, G.A., and Zane, L. 2011.
793 Genetic patchiness in European eel adults evidenced by molecular genetics and population

794 dynamics modelling. Mol. Phylogenet. Evol. **58**(2): 198–206.
795 doi:10.1016/j.ympev.2010.11.019.
796 Pujolar, J.M., Jacobsen, M.W., Als, T.D., Frydenberg, J., Munch, K., Jónsson, B., Jian, J.B., Cheng, L.,
797 Maes, G.E., Bernatchez, L., and Hansen, M.M. 2014. Genome-wide single-generation
798 signatures of local selection in the panmictic European eel. Mol. Ecol. **23**(10): 2514–2528.
799 doi:10.1111/mec.12753.
800 Railsback, S.F., and Harvey, B.C. 2013. Trait-mediated trophic interactions: is foraging theory keeping
801 up? Trends Ecol. Evol. **28**(2): 119–125. doi:10.1016/j.tree.2012.08.023.
802 Rougier, T., Lassalle, G., Drouineau, H., Dumoulin, N., Faure, T., Deffuant, G., Rochard, E., and
803 Lambert, P. 2015. The Combined Use of Correlative and Mechanistic Species Distribution
804 Models Benefits Low Conservation Status Species. PLOS ONE **10**(10): e0139194.
805 doi:10.1371/journal.pone.0139194.
806 Scheiner, S.M. 1993. Genetics and Evolution of Phenotypic Plasticity. Annu. Rev. Ecol. Syst. **24**: 35–68.
807 Schlichting, C.D. 1986. The Evolution of Phenotypic Plasticity in Plants. Annu. Rev. Ecol. Syst. **17**(1):
808 667–693. doi:10.1146/annurev.es.17.110186.003315.
809 Sultan, S.E. 1987. Evolutionary Implications of Phenotypic Plasticity in Plants. *In* Evolutionary Biology.
810 *Edited by* M.K. Hecht, B. Wallace, and G.T. Prance. Springer US. pp. 127–178.
811 Tesch, F.-W. 2003. The eel. *In* 3rd ed. Blackwell Science, Oxford, UK.
812 Travis, J. 1994. Evaluating the adaptive role of morphological plasticity. *In* Ecological Morphology.
813 *Edited by* P. Wainwright and S. Reilly. University of Chicago Press. pp. 99–122.
814 Ulrik, M.G., Pujolar, J.M., Ferchaud, A.-L., Jacobsen, M.W., Als, T.D., Gagnaire, P.A., Frydenberg, J.,
815 Bøcher, P.K., Jónsson, B., Bernatchez, L., and others. 2014. Do North Atlantic eels show
816 parallel patterns of spatially varying selection? BMC Evol. Biol. **14**(1): 138.
817 Varley, C.G., Gradwell, G.R., and Hassell, M.P. 1973. Insect population ecology an analytical approach.
818 University of California Press, California.
819 Vélez-Espino, L.A., and Koops, M.A. 2010. A synthesis of the ecological processes influencing variation
820 in life-history and movement patterns of American eel: towards a global assessment. Rev.
821 Fish Biol. Fish. **20**(2): 163–186. doi:10.1007/s11160-009-9127-0.
822 Vollestad, L.A. 1992. Geographic Variation in Age and Length at Metamorphosis of Maturing
823 European Eel: Ennvironmental Effects and Phenotypic Plasticity. J. Anim. Ecol. **61**(1): 41–48.
824 Weiner, J. 1990. Asymmertic Competition in Plant Population. Tree **5**(11): 360–364.
825 Williams, G.C. 1996. Adaptation and natural selection: a critique of some current evolutionary
826 thought. Princeton Univ. Press, Princeton, NJ.
827

828 **Tables**

829 **Table 1.** GenEveel parameter descriptions with reference values and modalities (- and +) for the 17

830 parameters involved in the experimental design.

| Parameter | Description | Reference value | (-) modality | (+) modality | Reference |
|---|---|---|---|---|---|
| *n* | Cells of river catchment | 30 | 24 | 36 | (Drouineau et al. 2014) |
| *N* | Number of glass eels that colonize freshwater | 30 000 | 24 000 | 36 000 | (Drouineau et al. 2014) |
| *a1* | Regression coefficient from fecundity at length | 8 846 | - | - | (Andrello et al. 2011) |
| *a* | Regression coefficient from fecundity at length | 1.3877119 | - | - | (Melià et al. 2006, Andrello et al. 2011) |
| *b* | Regression exponent from fecundity at length | 3.22 | 2.576 | 3.864 | (Melià et al. 2006) |
| $L_\infty$ (cm) | Asymptotic length | 76.2 | 60.96 | 91.44 | (De Leo and Gatto 1995) |
| $L_{sm}$ (cm) | Male length at silvering | 40.5 | 38.15 | 42.85 | (Vollestad 1992) |
| $L_g$ (cm) | Length at recruitment | 7.5 | 6 | 9 | (Desaunay and Guerault 1997, Dekker 1998, Desaunay et al. 2012) |
| *fertility* | Constant of male fertility | 43 | 40.5 | 45.5 | - |
| $K_{fast}(i,1)$, year$^{-1}$ | Fast intrinsic growth rate | 0.315 | 0.295 | 0.335 | (De Leo and Gatto 1995) |
| $K_{slow}(i,1)$, year$^{-1}$ | Slow intrinsic growth rate | 0.253 | 0.233 | 0.273 | (De Leo and Gatto 1995) |
| *propK* | Proportion of individuals that grow slowly | 0.5 | 0.4 | 0.6 | - |
| $M_{fast}(i,1)$, year$^{-1}$ | Fast intrinsic mortality rate | 0.38 | 0.405 | 0.355 | - |
| $M_{slow}(i,1)$, year$^{-1}$ | Slow intrinsic mortality rate | 0.138 | 0.15 | 0.127 | (Dekker 2000) |
| $\alpha$ | Intensity of density-dependence | 0.0001 | 0.00008 | 0.00012 | (Drouineau et al. 2014) |
| $r_K$ | Ratio between upstream and downstream growth rate | 0.5 | 0.4 | 0.6 | (Drouineau et al. 2014) |
| $r_M$ | Ratio between upstream and downstream mortality | 1 | 0.8 | 1.02 | (Drouineau et al. 2014) |

| | | | | | |
|---|---|---|---|---|---|
| | rate | | | | |
| $Y_K$ | Shape parameter of growth | 0.05 | 0.049 | 0.051 | (Drouineau et al. 2014) |
| $Y_M$ | Shape parameter of mortality | 0.05 | 0.049 | 0.051 | (Drouineau et al. 2014) |

831

832 **Table 2.** Results of Mann-Kendall test of reference simulation.

| Spatial pattern | Tau |
|---|---|
| Abundance | -1 |
| Mean length at silvering | 0.98 |
| Sex ratio (proportion of females) | 0.57 |
| Ratio of fast growers | -0.78 |
| Mean realized growth rate | -1 |

833

834 **Table 3.** Number of simulations with consistent patterns for each modality of the groups of
835 parameters, over the number of simulations for which it was possible to calculate a pattern. The
836 columns represent the spatial patterns and the numbers of simulations for which it was possible to
837 estimate a pattern.

| Parameters group | **Abundance 2560** | **Mean length at silvering 1920** | **Sex ratio (proportion of females) 1610** | **Ratio of fast growers 2560** | **Mean realized growth rate 2560** | **The five spatial patterns 1610** |
|---|---|---|---|---|---|---|
| ***N*** | (-) 1280/1280<br>(+) 1280/1280 | (-) 650/960<br>(+) 650/960 | (-) 70/800<br>(+) 60/810 | (-) 1280/1280<br>(+) 1280/1280 | (-) 1280/1280<br>(+) 1280/1280 | (-) 70/800<br>(+)60/810 |
| ***fertility*** and $L_{sm}$ | (-) 1280/1280<br>(+) 1280/1280 | (-) 800/960<br>(+) 500/960 | (-) 130/800<br>(+) 0/810 | (-) 1280/1280<br>(+) 1280/1280 | (-) 1280/1280<br>(+) 1280/1280 | (-)130/800<br>(+) 0/810 |
| $K_{fast}(i, 1)$ and $M_{fast}(i, 1)$ | (-) 1280/1280<br>(+) 1280/1280 | (-) 650/960<br>(+) 650/960 | (-) 70/810<br>(+) 60/800 | (-) 1280/1280<br>(+) 1280/1280 | (-) 1280/1280<br>(+) 1280/1280 | (-) 70/810<br>(+) 60/800 |
| $K_{slow}(i, 1)$ and $M_{slow}(i, 1)$ | (-) 1280/1280<br>(+) 1280/1280 | (-) 710/960<br>(+) 590/960 | (-) 0/810<br>(+) 130/800 | (-) 1280/1280<br>(+) 1280/1280 | (-) 1280/1280<br>(+) 1280/1280 | (-) 0/810<br>(+) 130/800 |
| ***propK*** | (-) 1280/1280<br>(+) 1280/1280 | (-) 650/960<br>(+) 650/960 | (-) 90/810<br>(+) 40/800 | (-) 1280/1280<br>(+) 1280/1280 | (-) 1280/1280<br>(+) 1280/1280 | (-) 90/810<br>(+) 40/800 |
| ***α*** | (-) 1280/1280<br>(+) 1280/1280 | (-) 810/960<br>(+) 490/960 | (-) 60/960<br>(+) 70/650 | (-) 1280/1280<br>(+) 1280/1280 | (-) 1280/1280<br>(+) 1280/1280 | (-) 60/960<br>(+) 70/650 |
| ***n*** | (-) 1280/1280<br>(+) 1280/1280 | (-) 660/960<br>(+) 640/960 | (-) 60/810<br>(+) 70/800 | (-) 1280/1280<br>(+) 1280/1280 | (-) 1280/1280<br>(+) 1280/1280 | (-) 60/810<br>(+) 70/800 |
| ***b*** | (-) 1280/1280<br>(+) 1280/1280 | (-) 360/640<br>(+) 940/1280 | (-) 10/640<br>(+) 120/970 | (-) 1280/1280<br>(+) 1280/1280 | (-) 1280/1280<br>(+) 1280/1280 | (-) 10/640<br>(+) 120/970 |
| $L_\infty$ | (-) 1280/1280<br>(+) 1280/1280 | (-) 310/640<br>(+) 990/1280 | (-) 120/640<br>(+) 10/970 | (-) 1280/1280<br>(+) 1280/1280 | (-) 1280/1280<br>(+) 1280/1280 | (-) 120/640<br>(+) 10/970 |
| $L_g$ | (-) 1280/1280<br>(+) 1280/1280 | (-) 650/960<br>(+) 650/960 | (-) 60/800<br>(+) 70/810 | (-) 1280/1280<br>(+) 1280/1280 | (-) 1280/1280<br>(+) 1280/1280 | (-) 60/800<br>(+) 70/810 |
| $r_k$ and $r_m$ | (-) 1280/1280<br>(+) 1280/1280 | (-) 630/960<br>(+) 670/960 | (-) 40/810<br>(+) 90/800 | (-) 1280/1280<br>(+) 1280/1280 | (-) 1280/1280<br>(+) 1280/1280 | (-) 40/810<br>(+) 90/800 |
| $\gamma_k$ and $\gamma_m$ | (-) 1280/1280<br>(+) 1280/1280 | (-) 730/960<br>(+) 570/960 | (-) 60/810<br>(+) 70/800 | (-) 1280/1280<br>(+) 1280/1280 | (-) 1280/1280<br>(+) 1280/1280 | (-) 60/810<br>(+) 70/800 |

838 **Table 4.** Results of the 13 combinations that generated five consistent patterns. The signs +/- refer to
839 the modalities of the parameters groups. The two last columns represent the five spatial patterns. An
840 ascendant arrows stands for positive Mann-Kendall tau value (increasing trend from downstream to
841 upstream). Conversely, a descendant arrow stands for a negative Mann-Kendall tau value.

| | $N$ | *fertility*, $L_{sm}$ | $K_{fast}(i, 1)$, $M_{fast}(i, 1)$ | $K_{slow}(i, 1)$, $M_{slow}(i, 1)$ | *propK* | $\alpha$ | $n$ | $b$ | $L_\infty$ | $L_g$ | $r_K$, $r_M$ | $\gamma_K$, $\gamma_M$ | **Abundance Ratio of fast growers** $\overline{K(t,x)}$ | **Sex ratio** $\overline{Ls}$ |
|---|---|---|---|---|---|---|---|---|---|---|---|---|---|---|
| 1 | - | - | - | + | + | + | + | + | - | - | + | + | ↘ | ↗ |
| 2 | + | - | - | + | - | + | + | + | - | + | + | + | ↘ | ↗ |
| 3 | + | - | - | + | + | - | + | + | - | + | + | - | ↘ | ↗ |
| 4 | - | - | - | + | - | - | + | + | - | - | + | - | ↘ | ↗ |
| 5 | + | - | + | + | + | - | - | + | - | - | + | - | ↘ | ↗ |
| 6 | + | - | - | + | - | - | - | + | - | + | - | - | ↘ | ↗ |
| 7 | - | - | - | + | - | + | + | - | + | + | + | + | ↘ | ↗ |
| 8 | - | - | + | + | - | - | - | + | - | + | + | - | ↘ | ↗ |
| 9 | - | - | + | + | + | + | - | + | - | + | + | + | ↘ | ↗ |
| 10 | - | - | + | + | - | + | + | + | - | + | - | + | ↘ | ↗ |
| 11 | + | - | + | + | - | + | - | + | - | - | + | + | ↘ | ↗ |
| 12 | - | - | - | + | - | + | - | + | - | - | - | + | ↘ | ↗ |
| 13 | + | - | + | + | - | - | + | + | - | - | - | - | ↘ | ↗ |

842

**Figures**

**Fig. 1.** Flow chart representing the fish biological pathway.

**Fig. 2.** Algorithm of the model GenEveel.

**Fig. 3.** Output values for the five spatial patterns resulting from the reference simulation.

**Fig. 4.** Simulated mean length at silvering patterns in the 13 combinations of parameters that consistently mimic the pattern described in the literature. These 13 combinations correspond to the 13 combinations that generate consistent patterns for all the five spatial patterns. Each plot stands for a combination (the number is an identifier of the combination that can be found in table 4) and each line stands for a replicate.

**Fig. 5.** Simulated sex ratio (proportions of females) patterns in the 13 combinations of parameters that consistently mimic the pattern described in the literature. These 13 combinations correspond to the 13 combinations that generate consistent patterns for all the five spatial patterns. Each plot stands for a combination (the number is an identifier of the combination that can be found in table 4) and each line stands for a replicate.

857 **Supplemental Information**

858 **Table S1.** Results of the 256 combinations. The signs +/- refer to the modalities of the parameters
859 groups . The last five columns represent the spatial patterns. An ascendant arrows stands for positive
860 Mann-Kendall tau value (increasing trend from downstream to upstream). Conversely, a descendant
861 arrow stands for a negative Mann-Kendall tau value.

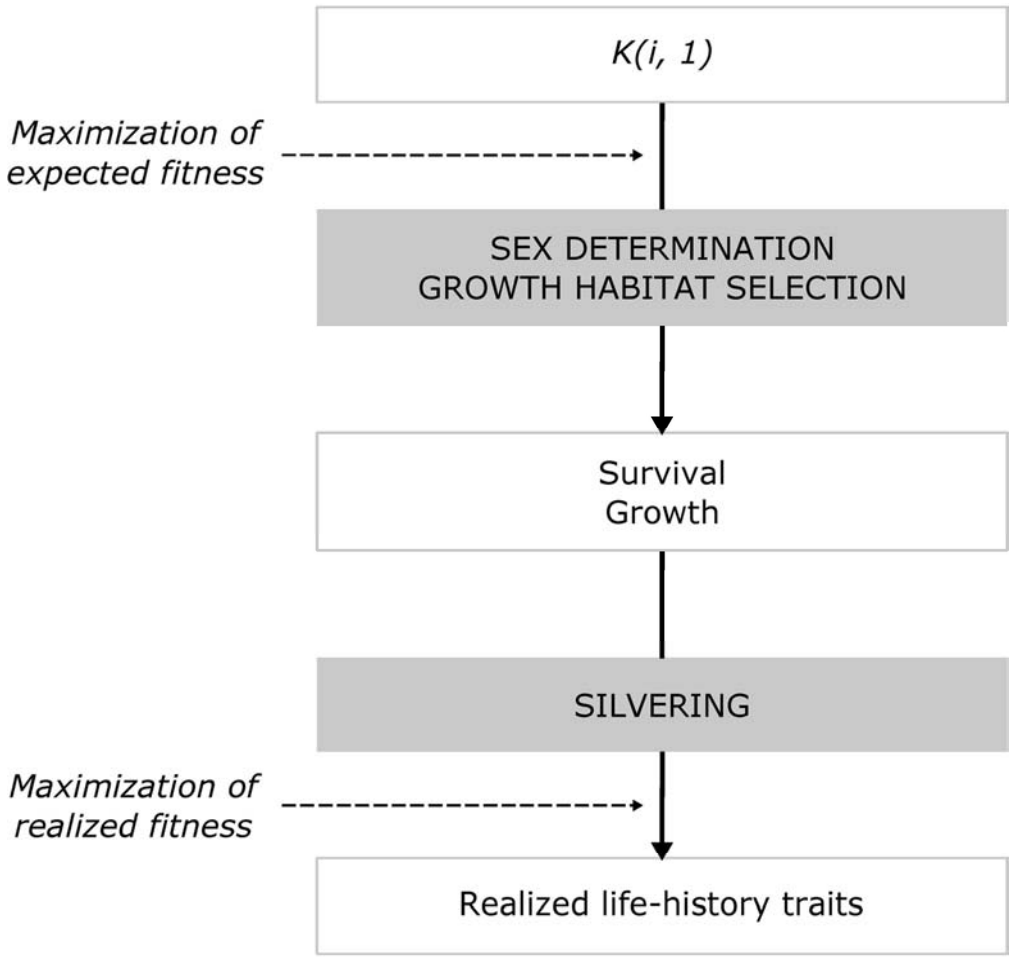


Fig. 1. Flow chart representing the fish biological pathway.

117x112mm (300 x 300 DPI)

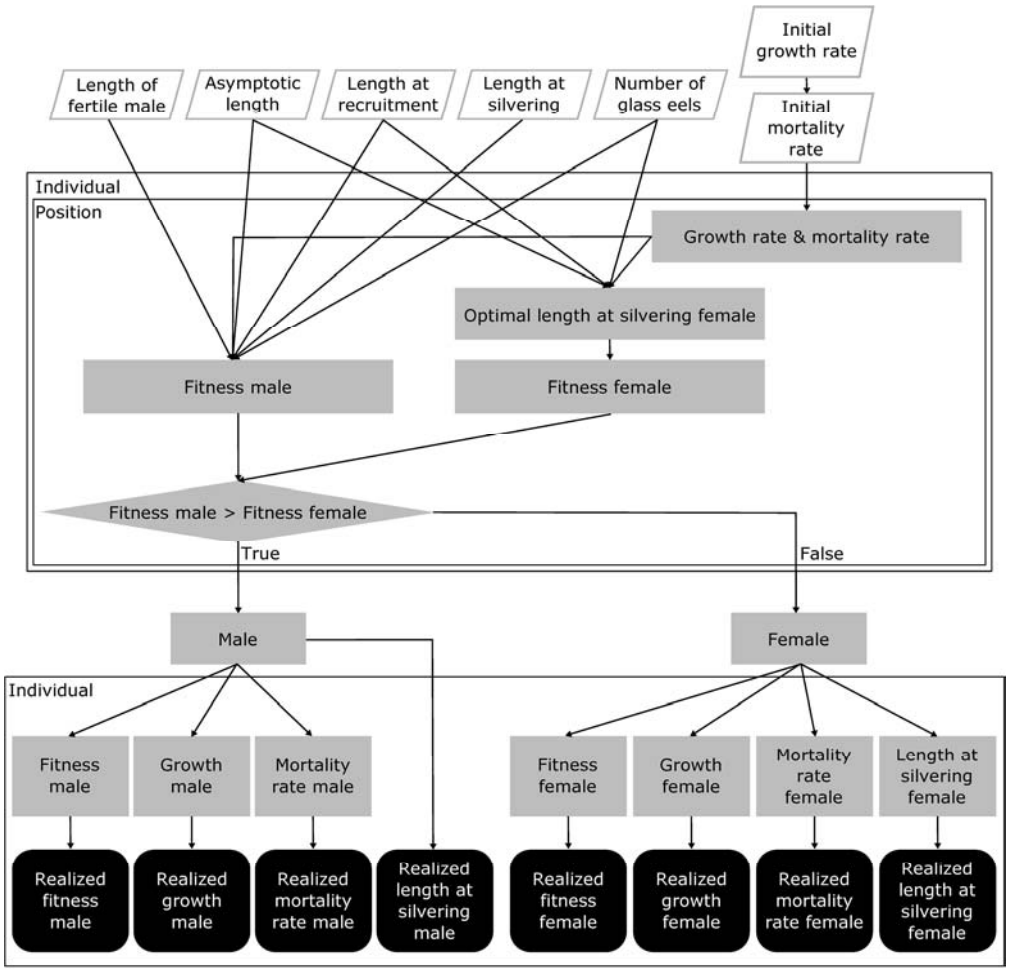


Fig. 2. Algorithm of the model GenEveel.

198x191mm (300 x 300 DPI)

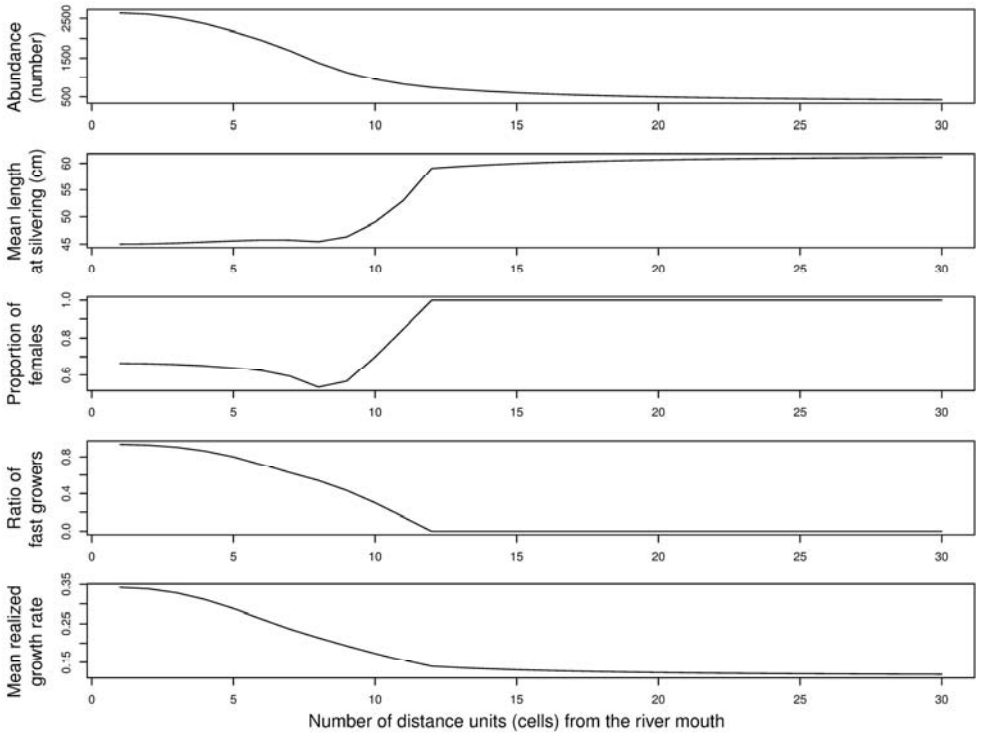


Fig. 3. Output values for the five spatial patterns resulting from the reference simulation.

182x141mm (300 x 300 DPI)

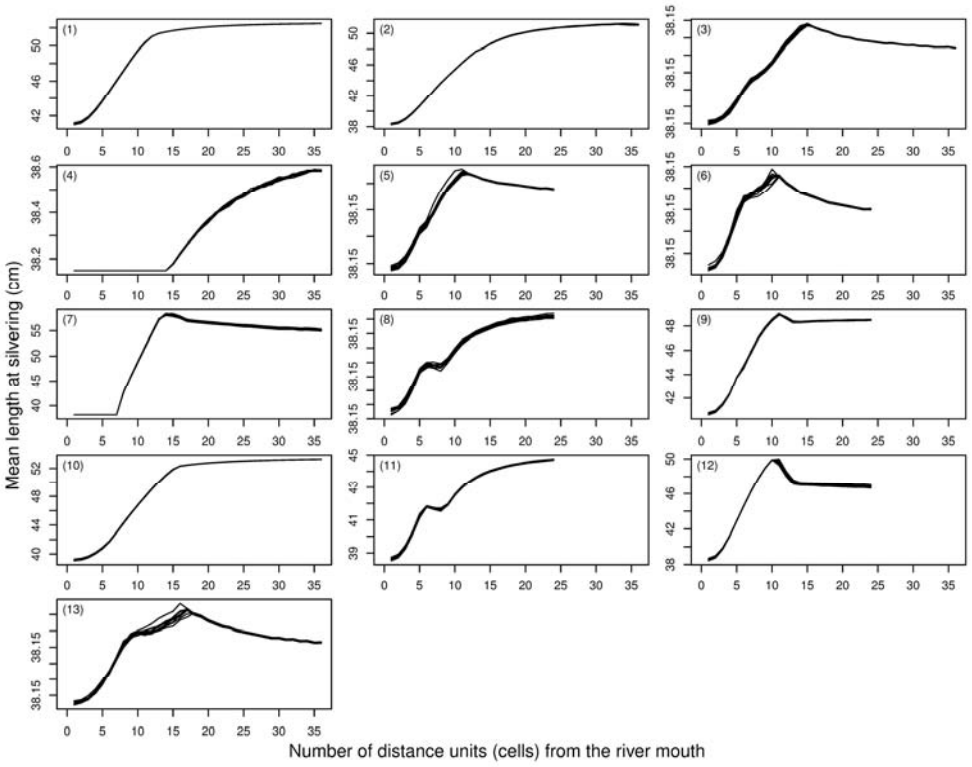


Fig. 4. Simulated mean length at silvering patterns in the 13 combinations of parameters that consistently mimic the pattern described in the literature. These 13 combinations correspond to the 13 combinations that generate consistent patterns for all the five spatial patterns. Each plot stands for a combination (the number is an identifier of the combination that can be found in table 4) and each line stands for a replicate.

182x141mm (300 x 300 DPI)

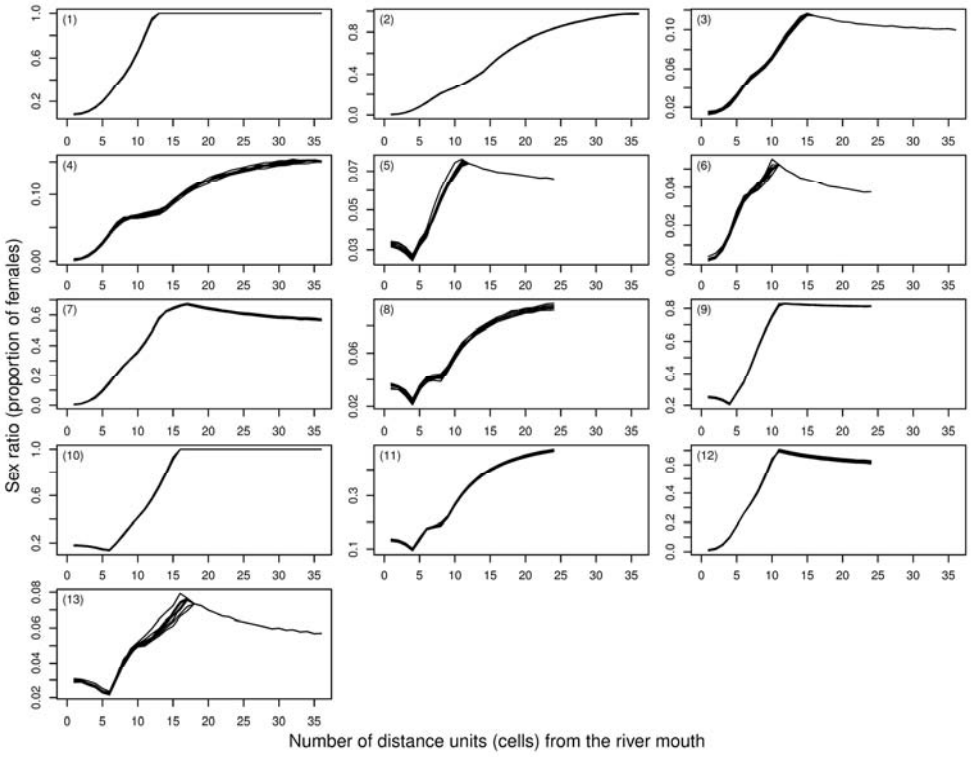


Fig. 5. Simulated sex ratio (proportions of females) patterns in the 13 combinations of parameters that consistently mimic the pattern described in the literature. These 13 combinations correspond to the 13 combinations that generate consistent patterns for all the five spatial patterns. Each plot stands for a combination (the number is an identifier of the combination that can be found in table 4) and each line stands for a replicate.

182x141mm (300 x 300 DPI)